## PAPER

Check for updates

# Hybridization of nanofiber-modified fabrics with porphyrin-based nanosheets for nanoparticle capture†

Yusuke Kuramochi, [ID] [a] Yuna Aoki,[a] Kyoko Enomoto,[a] Seiji Nakamura,[a] Hideyuki Tanaka,[b] Keiichiro Ozawa,[b] Miki Hasegawa, [ID] [b] Osamu Ohsawa,[cd] Kei Watanabe [ID] *[cd] and Kazuyuki Ishii [ID] *[a]

Nanoporous filters covering large areas and exhibiting high strength are crucial for capturing small particles, such as viruses. However, the direct capture of nanoparticles requires the layering of numerous fibers, which significantly obstructs air flow. In this study, nanofiber-modified non-woven fabrics are hybridized with two-dimensional porphyrin-based nanosheets. Obtained through the interfacial reaction of a toluene/$n$-hexanol solution of 5,10,15,20-tetrakis(4-carboxyphenyl)porphyrin with a $CuCl_2$ aqueous solution, the nanosheets feature regular nanopores of a few nanometres. Hybridization is achieved by stamping nanofiber-modified non-woven fabrics onto large-area porphyrin-based nanosheets, covering the mesoporous meshes of the nanofibers with nanopores. Moreover, this coverage is optimized by using nanosheets compressed to different degrees. These hybridized filters capture particles of several tens of nanometres, which are smaller than viruses in size, with a minimal drop in the differential pressure. This study demonstrates not only the utility of molecular nanosheets but also a new approach for hybridizing nanofiber-modified non-woven fabrics.

## 1. Introduction

The global COVID-19 pandemic has highlighted the importance of filters, including face masks, for removing micro-aerosol droplets containing viruses.[1] Non-woven fabrics have been widely used as filters owing to their cost-effectiveness and ease of manufacturing. Nanofibers with cross-sectional diameters ranging from tens to hundreds of nanometres have a high area-to-volume ratio, and layering nanofibers produces fine porous meshes. One of the versatile methods for manufacturing nanofibers is electrospinning based on electrohydrodynamics.[2,3] Filters fabricated by layering electrospun nanofibers on non-woven fabrics efficiently capture particles such as bacteria (approximately 1 μm) and PM2.5 (2.5 μm)[4] owing to the sub-micrometre pores of the nanofiber layers. Consequently, these

nanofibers can remove μm-sized fine particles without obstructing air flow. However, to directly capture small particles such as viruses, including COVID-19 (60–140 nm),[5] numerous additional layers are required. This results in a significant drop in the differential pressure, which in face masks, can be a source of discomfort to the wearer.

Nanosheets based on two-dimensional metal–organic frameworks have attracted considerable attention for their potential application in gas separation, energy conversion and storage, catalysis, sensors, and biomedicine.[6–8] Porphyrins featuring a rigid, π-conjugated planar structure with four-fold symmetrical ligands are promising candidates for constructing grid structures. Makiura *et al.* used the Langmuir–Blodgett (LB) method to prepare highly ordered porphyrin nanosheets in which the free-base or metal(II) 5,10,15,20-tetrakis(4-carboxyphenyl)porphyrins (MTCPP, M = $H_2$, Co, and Pd) is bridged by paddle-wheel linkages to two Cu(II) ions and four carboxylate groups.[9–12] To prepare cobalt porphyrin-based nanosheets, a chloroform–methanol solution containing CoTCPP and pyridine is spread on a $CuCl_2$ aqueous solution, resulting in a regular two-dimensional structure with well-defined nanopores on the water surface.[9,10] The same group also prepared free-base porphyrin nanosheets by spreading a toluene/ethanol solution of the porphyrin on a $CuCl_2$ aqueous solution.[11] The nanosheets are layered on silicon, quartz, and gold substrates

[a] Institute of Industrial Science, The University of Tokyo, 4-6-1 Komaba, Meguro-ku, Tokyo 153-8505, Japan. E-mail: k-ishii@iis.u-tokyo.ac.jp

[b] College of Science and Engineering, Aoyama Gakuin University, 5-10-1 Fuchinobe, Chuo-ku, Sagamihara, Kanagawa 252-5258, Japan

[c] NafiaS Inc., Fii building, Shinshu University (Ueda Campus), 3-15-1 Tokida, Ueda, Nagano 386-8567, Japan. E-mail: k.watanabe@nafias-jp.com

[d] Nano Fusion Research Group, Institute for Fiber Engineering and Science (IFES), Shinshu University, 3-15-1 Tokida, Ueda, Nagano 386-8567, Japan

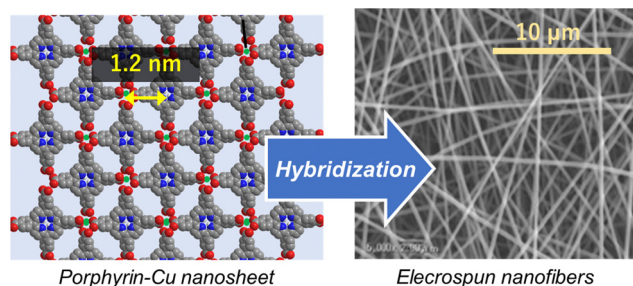† Electronic supplementary information (ESI) available. See DOI: https://doi.org/10.1039/d5ma00058k

**Fig. 1** Schematic illustration of a porphyrin-based nanosheet (H atoms are omitted for clarity) and scanning electron microscopy (SEM) image of electrospun polyurethane nanofibers.

to form highly crystalline nanofilms. These nanosheets have regular nanopores of a few nanometres (Fig. 1 and Fig. S1, ESI†),[9–12] and thus they are promising filters for removing nm-sized particles. However, their limited mechanical strength is a disadvantage in high-stress environments such as filtration systems.

Herein, to develop filters capable of capturing nano-particles without restricting airflow, we hybridized electrospun polyurethane nanofibers on wet-laid polyethylene terephthalate non-woven fabrics with porphyrin-based nanosheets (Fig. 1). The porphyrin-based nanosheets provide nanopores that are permeable to air (Fig. S2, ESI†). Hybridization was conducted to reinforce the porphyrin-based nanosheets as well as to add nanopores to the mesoporous meshes of the nanofiber-based layers. First, we prepared large-area porphyrin-based nanosheets, which were subsequently assembled onto nanofiber-modified fabrics, affording reinforced nanosheet filters on the scale of centimetres. We used scanning electron microscopy (SEM) to show that porphyrin-based nanosheets covered the mesoporous meshes of the nanofiber-based layers. Measurements of the pressure differential and particle filtration efficiency showed that the hybridized non-woven fabrics captured nanoparticles (100 nm) smaller than typical viruses with a minimal drop in the differential pressure.

## 2. Experimental

### 2.1. Materials

All chemicals and solvents were used without further purification unless otherwise stated. 5,10,15,20-Tetrakis(4-carboxyphenyl)porphyrin ($H_2$TCPP) (Sigma-Aldrich, St Louis, MO, USA) and $CuCl_2$ (FUJIFILM Wako Chemicals, Osaka, Japan) were reagent grade. Toluene (KANTO Chemicals, Tokyo, Japan) and n-hexanol (FUJIFILM Wako Chemicals, Osaka, Japan) were special grade.

### 2.2. Surface morphology

The surface morphologies of bare and hybridized fabrics were investigated using SEM (VE-9800, KEYENCE, Osaka, Japan).

### 2.3. Preparation of porphyrin nanosheets using $CuCl_2$ ($H_2$TCPP-Cu) for transmittance and evanescent wave absorption spectroscopy

First, 250 μL of 0.2 mM $H_2$TCPP in a mixed solvent of toluene and n-hexanol (3 : 1 v/v) was added to 100 mM $CuCl_2$ aqueous solution (250 mL) in a petridish ($\phi$ 20 cm) using a micro-syringe. The resulting layer was allowed to stand for 30 min to evaporate the organic solvents. The $CuCl_2$ aqueous solution was replaced with MilliQ water (total 2.5 L) to remove an excess of $CuCl_2$, because they form precipitates when porphyrin-based nanosheets were transferred onto glass substrates. A glass substrate (76 × 26 mm) was immersed in the water surface on which the $H_2$TCPP-Cu nanosheet had been formed, and then slowly lifted up to transfer the nanosheet onto the glass substrate. Transmittance absorption spectra of the nanosheets were measured at room temperature with a spectrophotometer (V-570, JASCO, Tokyo, Japan). Evanescent wave absorption spectra of the nanosheets were measured as described in a previous report.[13] A halogen lamp (FHL-102, Asahi Spectra, Tokyo, Japan) equipped with a polarizer (Sigmakoki, Tokyo, Japan) was used to provide s-polarized light with an electric field perpendicular to the glass substrate and p-polarized light with an electric field parallel to the glass substrate. A multi-channel spectrophotometer (MSP-1000, Unisoku, Osaka, Japan) was used as the detector.

### 2.4. Surface pressure–molecular area (π–A) isotherm measurements

First, 2 L of 100 mM $CuCl_2$ aqueous solution was put in a trough whose surface area is movable (50 × 5 × 8 cm, Filgen, Nagoya, Japan). Subsequently, 60 μL of 0.2 mM $H_2$TCPP in a mixed solvent of toluene and n-hexanol (3 : 1 v/v) was slowly spread on the $CuCl_2$ aqueous solution at three spots in the trough. The resulting layers were allowed to stand for 1 h to evaporate the organic solvents, and then, surface pressure–molecular area isotherms were acquired at room temperature using a two-barrier continuous pressing speed of 15 mm min$^{-1}$.

### 2.5. Preparation of nanofiber-modified fabrics

Polyurethane nanofibers (0.5 g m$^{-2}$) were directly spun onto 30 g m$^{-2}$ wet-laid polyethylene terephthalate non-woven fabrics using a multi-nozzle electrospinning device (NafiaS, Nagano, Japan).[3] Before electrospinning, the fabrics were treated by heat-pressing to decrease irregularities. The spinning solution of polyurethane nanofibers was prepared by dissolving polyurethane resin in a mixed solvent of N,N-dimethylformamide (DMF) and methyl ethyl ketone at a ratio of 7 : 3 and concentration of 10 wt% with stirring for 24 h at room temperature.

### 2.6. Hybridization of nanofiber-modified fabrics with porphyrin-based nanosheets

For hybridization with uncompressed nanosheets, 700 mL of 100 mM $CuCl_2$ aqueous solution was put in a polyvinyl chloride (PVC) pad (20 × 25 cm). Then, 600 μL of 0.2 mM $H_2$TCPP in a mixed solvent of toluene and n-hexanol (3 : 1 v/v) was added

dropwise onto the CuCl$_2$ aqueous solution. The resulting layer was allowed to stand for 30 min to evaporate the organic solvents. The CuCl$_2$ aqueous solution was replaced with MilliQ water (total 5.1 L) using two peristaltic pumps (Front Lab, AS ONE, Osaka, Japan). Wet-laid polyethylene terephthalate non-woven fabrics (15 × 15 cm) covered by layers of polyurethane nanofibers were stamped onto porphyrin-based nanosheets. For hybridization with manually compressed nanosheets, 600 μL of 0.2 mM H$_2$TCPP in a mixed solvent of toluene and n-hexanol (3 : 1 v/v) was added dropwise onto 700 mL of 100 mM CuCl$_2$ aqueous solutions in PVC pads (20 × 25 cm). The resulting layers were allowed to stand for 30 min to evaporate the organic solvents. Porphyrin-based nanosheets were compressed to 2/3 and 1/3 of their original horizontal length at a speed of 1 cm min$^{-1}$. Wet-laid polyethylene terephthalate non-woven fabrics (5 × 5 cm) covered by layers of polyurethane nanofibers were stamped onto porphyrin-based nanosheets. For hybridization with nanosheets precisely compressed using a trough, 2.0 L of 100 mM CuCl$_2$ aqueous solution was placed in the movable range of a trough (50 × 5 × 8 cm). Subsequently, 60 μL of 0.2 mM H$_2$TCPP in a mixed solvent of toluene and n-hexanol (3 : 1 v/v) was slowly spread on the CuCl$_2$ aqueous solution at three spots in the trough. The resulting layer was allowed to stand for 1 h to evaporate the organic solvents. The layer was compressed until the molecular area was 200 Å$^2$, and then wet-laid polyethylene terephthalate non-woven fabrics (4 × 4 cm) covered by layers of polyurethane nanofibers were stamped onto porphyrin-based nanosheets on CuCl$_2$ aqueous layers. The composite was immersed in pure water for 5 min to leach out an excess of CuCl$_2$, and then dried.

### 2.7. Measurements of differential pressure and particle filtration efficiency

We conducted tests using a filter testing apparatus capable of performing evaluations in accordance with the standard test method for N95 filters. The differential pressure and filtration efficiency were measured using the NaCl aerosol method with a filter tester employed for particulate respirators (AP-632F, Sibata Scientific Technology, Saitama, Japan). First, 2% (wt/vol) NaCl solution was aerosolized, passed through the convex side of a test sample, properly sealed, and placed into a filter holder. The particle size ranged from 0.022 to 0.259 μm with a count median diameter of 0.075 ± 0.020 μm and geometric standard deviation of less than 1.86. The concentrations of the NaCl aerosol upstream and downstream of the sample (area of 3 × 3 cm) were measured at a flow rate of 16.7 L min$^{-1}$ for 1 min. The filtration efficiency was estimated using eqn (1):

Filtration efficiency (%)

$$= \left\{ 1 - \frac{N(\text{Particle concentration downstream})}{N(\text{Particle concentration upstream})} \times 100 \right\} \quad (1)$$

where $N$(upstream side particle concentration) and $N$(downstream side particle concentration) are the concentration of particles before and after filtering, respectively.

# 3. Results and discussion

## 3.1. Preparation and characterization of porphyrin-based nanosheets

Porphyrin-based nanosheets were prepared according to previously reported methods[9,11] with modification. Specifically, an organic solution containing 0.2 mM H$_2$TCPP was added to a CuCl$_2$ aqueous solution using a micro-syringe, producing a porphyrin-based nanosheet as a brown layer on the aqueous solution. In previous methods, a mixture of chloroform and methanol (3 : 1 v/v)[9] or a mixture of toluene and ethanol (1 : 1 v/v)[11] was used as the organic solvent. In the present method, toluene and n-hexanol (3 : 1 v/v) was employed as the mixed solvent to increase the area of porphyrin-based nanosheets. Herein, H$_2$TCPP does not dissolve in toluene (chloroform), but is soluble in n-hexanol (methanol). Therefore, the optimal combination of toluene, which does not sink in water, and n-hexanol, which dissolves H$_2$TCPP, enables the organic layer to spread on the aqueous solution. Furthermore, the concentration of CuCl$_2$ aqueous solution was increased from 1 mM to 100 mM, to accelerate the interfacial reaction between Cu(ıı) ions and the carboxylate moieties of H$_2$TCPP. As a result, the kinetics of interfacial complexation were controlled to prepare cm-ordered porphyrin-based nanosheets.

Fig. 2 shows the transmittance absorption and evanescent wave absorption spectra of porphyrin-based nanosheets transferred onto glass substrates. Here, to reduce light scattering from precipitates of CuCl$_2$ (Fig. S3, ESI†), excess Cu(ıı) ions in
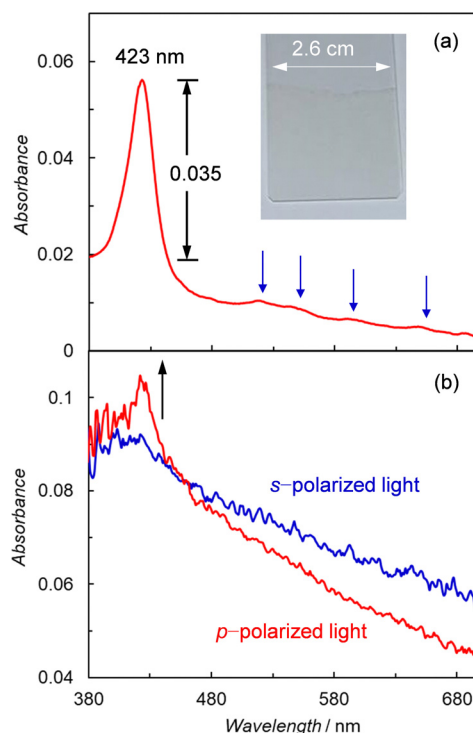


**Fig. 2** (a) Transmittance absorption and (b) polarized evanescent wave absorption spectra of porphyrin-based nanosheets on glass substrates. The blue arrows indicate the four peaks in the Q band region.

the aqueous solution were removed by replacing the $CuCl_2$ aqueous solution with pure water. Subsequently, nanosheets were transferred onto glass substrates, producing a pale-yellow layer on them (inset of Fig. 2a). The UV-vis absorption spectrum of a pale-yellow glass substrate (Fig. 2a) contained a Soret band and four Q bands, indicating that the pale-yellow color was derived from the $H_2TCPP$ chromophore. The sharp Soret band indicated that the $H_2TCPP$ chromophore did not stack on the glass substrate. Additionally, the four Q band peaks indicated that few Cu ions were inserted into the porphyrin center during the formation of nanosheets. The absorbance (0.035) of the Soret band after subtracting the baseline (Fig. 2a) corresponds to that of the monolayer, as reported in the literature.[11] This confirms that the nanosheets formed on the water surface are the monolayer. The s- and p-polarized spectra were observed by the lights whose electric fields were perpendicular and parallel to the glass substrate, respectively.[13] As shown in Fig. 2b, the Soret band clearly appeared only in the p-polarized absorption spectrum, indicating that the $H_2TCPP$ plane of the nanosheets was oriented parallel to the glass substrate.

To investigate the molecular orientation and coordination of porphyrin-based nanosheets, surface pressure–molecular area ($\pi$–A) isotherms were acquired (Fig. 3). The surface pressure rose steeply at the molecular area of approximately 180 Å$^2$ (equivalent to the planar area of $H_2TCPP$), indicating that the hydrophobic porphyrin rings were oriented horizontally relative to the aqueous solution surface. As the control experiments, $H_2TCPP$-based layer was prepared on pure water. In the $\pi$–A isotherms of this layer (Fig. 3 inset), the surface pressure rose steeply at the molecular area of approximately 40 Å$^2$ (the cross-sectional area of $H_2TCPP$), which indicated that the porphyrin plane was perpendicular to the water surface, thereby hiding the hydrophobic porphyrin rings from the water surface. Even when using a Ca(II) aqueous solution instead of a Cu(II) solution, the same result as that with pure water was observed, supporting that the nanosheets had a paddle-wheel type

coordination of carboxylate groups to Cu(II) ions ($Cu_2(COO)_4$), similar to previous reports.[9–11]

When forming the porphyrin nanosheets, we observed interesting dynamics just after the porphyrin solution was dropped onto the $CuCl_2$ aqueous solution. When a droplet of toluene/n-hexanol solution containing $H_2TCPP$ was placed on the surface of 100 mM $CuCl_2$ aqueous solution, the droplet initially spread out concentrically. After an induction period of a few seconds, the spreading droplet suddenly exploded (Movie S1, ESI†). This explosion required both $H_2TCPP$ and $CuCl_2$. For example, the following combinations resulted in a slow random dispersion of the organic solution: (1) a droplet of toluene/n-hexanol solution with (Movie S2, ESI†) or without (Movie S3, ESI†) $H_2TCPP$ on pure water instead of $CuCl_2$ aqueous solution and (2) a droplet of toluene/n-hexanol solution without $H_2TCPP$ on 100 mM $CuCl_2$ aqueous solution. Additionally, the droplet containing $H_2TCPP$ did not explode when 1 mM $CuCl_2$ aqueous solution instead of 100 mM $CuCl_2$ aqueous solution was used. This suggests that rapid complexation is necessary for the explosion to occur. Rapid complexation between $H_2TCPP$ and Cu(II) ions generates a gradient of surface tensions, i.e., the Marangoni effect,[14,15] which enables interfacial explosion for the formation of large-area porphyrin-based nanosheets.

### 3.2. Hybridization of nanofiber-modified fabrics with porphyrin-based nanosheets

Similar to porphyrin-based nanosheets transferred onto glass substrates, nanosheets transferred onto nanofiber-modified fabrics were uniformly distributed, as indicated by the spread of the pale-yellow layer. To optimize the hybridization of nanofiber-modified fabrics with porphyrin-based nanosheets, we acquired SEM images of a bare nanofiber-modified non-woven fabric without hybridization (Fig. 4b) and a nanofiber-modified non-woven fabric hybridized with a porphyrin-based nanosheet (Fig. 4c). First, porphyrin-based nanosheets were formed by dropping and spreading a $H_2TCPP$ solution on $CuCl_2$ aqueous solution. Then, the layer of a porphyrin-based nanosheet was transferred directly onto a nanofiber-modified non-woven fabric. SEM images of this fabric showed many defective holes. As the area was manually reduced to increase the density of the nanosheet, films began to form on the nanofibers. The compression process contributes to the formation of a uniform membrane. Therefore, porphyrin-based nanosheets were precisely compressed using the Langmuir–Blodgett trough until the molecular area reached 200 Å$^2$. After confirming that the added porphyrin densely covered the water surface, the nanosheets were transferred onto nanofiber-modified fabrics ($4 \times 4$ cm) using the stamping method.[16] As a result, white nanofiber-modified fabrics were uniformly colored in pale-yellow after hybridization with porphyrin-based nanosheets (Fig. 4a). Furthermore, in contrast to bare nanofiber-modified fabrics, which had μm-sized pores only (Fig. 4b), hybridized fabrics had a uniform film covering the nanofiber-based pores (Fig. 4c). For the first time, nanofiber-modified fabrics were successfully hybridized with porphyrin-based nanosheets, which covered the nanofiber-based pores.
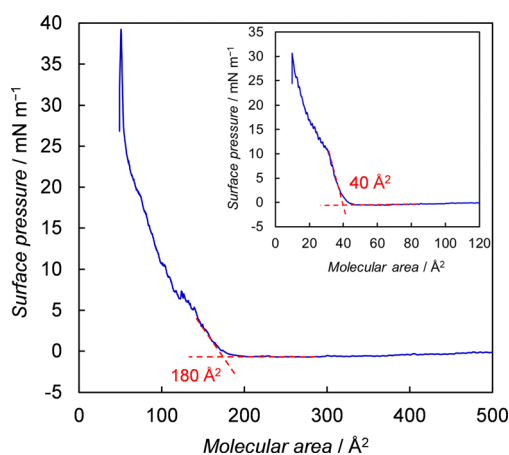


**Fig. 3** Surface pressure–molecular area ($\pi$–A) isotherm of $H_2TCPP$ on $CuCl_2$ (100 mM) aqueous solution. The inset shows the $\pi$–A isotherm of $H_2TCPP$ on pure water.
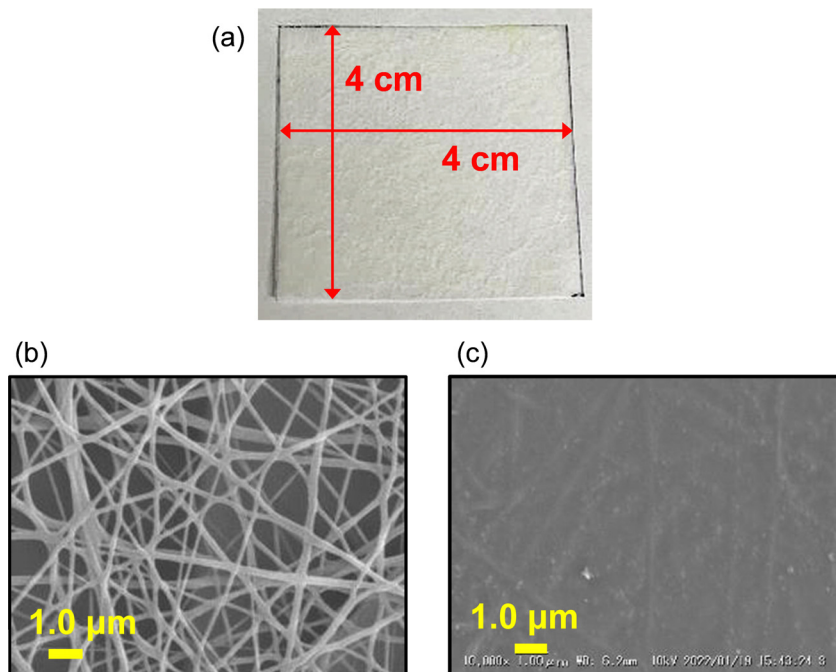
**Fig. 4** (a) Photograph of nanofiber-modified fabric hybridized with a porphyrin-based nanosheet. SEM images of nanofiber-modified fabrics before (b) and after (c) hybridization with a porphyrin-based nanosheet.

### 3.3. Filtration properties of nanosheet-hybridized nanofiber-modified fabrics

To evaluate the filtration properties of nanosheet-hybridized nanofiber-modified fabrics, the differential pressure was measured using a gas flow system. The differential pressure of fabrics hybridized with porphyrin-based nanosheets was evaluated to be 285 Pa, which was similar to that (256 Pa) of bare nanofiber-modified fabrics. Thus, the nm-sized pores of the nanosheets contribute to this minimal drop in the differential pressure. Furthermore, the filtration of NaCl particles in
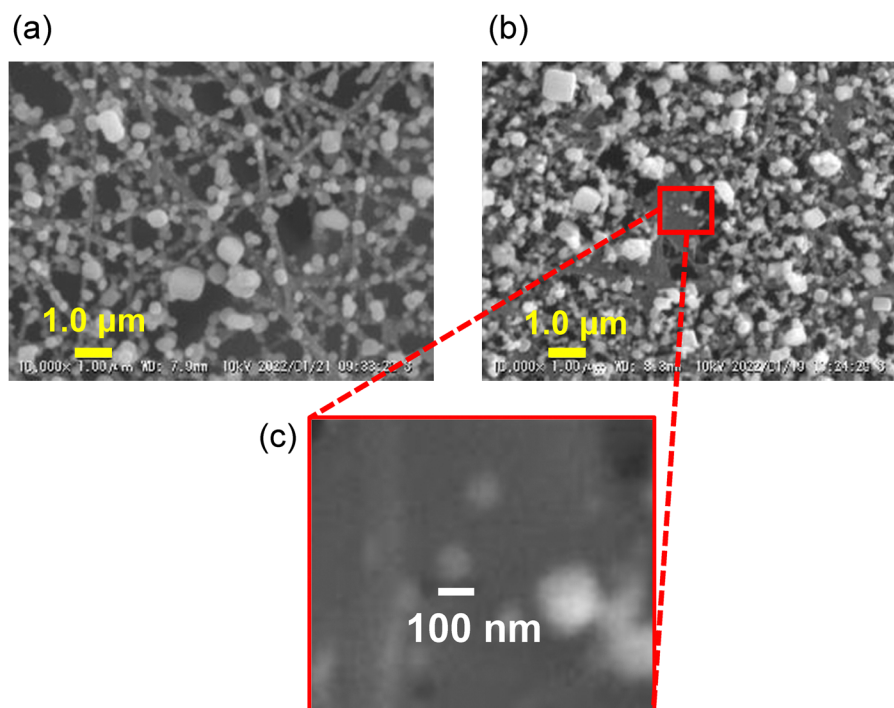


**Fig. 5** SEM images of nanofiber-modified fabrics without (a) and with (b) a porphyrin-based nanosheet after particle filtration tests. (c) Magnified view of a film-like porphyrin-based nanosheet.

flowing gas was examined. The particle filtration efficiency of nanofiber-modified fabrics hybridized with porphyrin-based nanosheets was evaluated to be $96.0 \pm 0.75\%$, which was larger than that of bare nanofiber-modified fabrics ($94.0 \pm 0.20\%$). Although the increase was only 2%, this improvement was considered to be significant because achieving such a value typically requires numerous additional electrospinning processes. Nanofiber-modified fabrics hybridized with porphyrin-based nanosheets without compression had defective holes on the film covering the nanofibers, and thus their particle filtration efficiency was similar to that of bare nanofiber-modified fabrics. This demonstrates the importance of compression using a Langmuir–Blodgett trough to produce a uniform film covering large-area of the nanofibers for filtering particles. We also formed double-layered nanosheets by laminating an additional compressed nanosheet onto the film formed using the stamping method, thereby increasing the differential pressure to 302 Pa and the particle filtration efficiency to 97.3%.

Fig. 5 shows the SEM images of nanofiber-modified fabrics after the particle filtration tests. The number of captured NaCl particles was larger in the nanofiber-modified fabric hybridized with a porphyrin-based nanosheet (Fig. 5b) than in the bare nanofiber-modified fabric (Fig. 5a). In particular, as shown in Fig. 5c, fabrics hybridized with porphyrin-based nanosheets captured particles (approximately 100 nm) that were smaller than viruses, i.e., influenza A[17] and COVID-19,[5] which are on the order of 100 nm in size. Thus, hybridization of nanofiber-modified fabrics with porphyrin-based nanosheets enabled the capture of particles less than 100 nm in size, showing great potential for the efficient capture of small particles such as viruses.

## 4. Conclusions

We prepared large-area porphyrin-based nanosheets by adding a mixed solvent of toluene and n-hexanol as the organic layer onto a concentrated $CuCl_2$ aqueous solution. A droplet of the porphyrin solution on the aqueous solution exploded after a short induction time to form a large-area porphyrin-based nanosheet. Hybridization of nanofiber-modified non-woven fabrics with porphyrin-based nanosheets compressed to different degree was achieved using the stamping method. Nanofiber-modified non-woven fabrics hybridized with porphyrin-based nanosheets captured particles of less than 100 nm in size with a minimal drop in the differential pressure. Thus, hybridization with nanosheets is a promising approach for producing non-woven filters capable of removing viruses and other small particles without a significant drop in the differential pressure.

## Author contributions

Y. K.: validation, writing – original draft. Y. A.: methodology, investigation. K. E.: methodology, investigation, data curation.

S. N.: investigation. H. T.: investigation. K. O.: investigation. M. H.: supervision, writing – review & editing. O. O.: investigation, visualization. K. W.: methodology, supervision, writing – review & editing. K. I.: conceptualization, project administration, supervision, writing – review & editing.

## Data availability

The data supporting this article have been included as part of the ESI.†

## Conflicts of interest

There are no conflicts to declare.

## Acknowledgements

## Notes and references

1 Y. Wibisono, C. R. Fadila, S. Saiful and M. R. Bilad, *Polymers*, 2020, **12**, 2516.
2 J. Xue, T. Wu, Y. Dai and Y. Xia, *Chem. Rev.*, 2019, **119**, 5298.
3 O. Ohsawa, G. Mayakrishnan, Y. Ge, C. Zhu, K. Watanabe and I. S. Kim, *Green Chem.*, 2023, **25**, 7556.
4 C. Liu, P.-C. Hsu, H.-W. Lee, M. Ye, G. Zheng, N. Liu, W. Li and Y. Cui, *Nat. Commun.*, 2015, **6**, 6205.
5 Y. M. Bar-On, A. Flamholz, R. Phillips and R. Milo, *eLife*, 2020, **9**, e57309.
6 M. Zhao, Y. Huang, Y. Peng, Z. Huang, Q. Ma and H. Zhang, *Chem. Soc. Rev.*, 2018, **47**, 6267.
7 G. Chakraborty, I. H. Park, R. Medishetty and J. J. Vittal, *Chem. Rev.*, 2021, **121**, 3751.
8 Y. Cheng, S. J. Datta, S. Zhou, J. Jia, O. Shekhah and M. Eddaoudi, *Chem. Soc. Rev.*, 2022, **51**, 8300.
9 R. Makiura, S. Motoyama, Y. Umemura, H. Yamanaka, O. Sakata and H. Kitagawa, *Nat. Mater.*, 2010, **9**, 565.
10 R. Makiura and H. Kitagawa, *Eur. J. Inorg. Chem.*, 2010, 3715.
11 S. Motoyama, R. Makiura, O. Sakata and H. Kitagawa, *J. Am. Chem. Soc.*, 2011, **133**, 5640.
12 R. Makiura and O. Konovalov, *Sci. Rep.*, 2013, **3**, 2506.
13 T. Shibanuma, R. Nakamura, Y. Hirakawa, K. Hashimoto and K. Ishii, *Angew. Chem., Int. Ed.*, 2011, **50**, 9137.
14 L. E. Scriven and C. V. Sternling, *Nature*, 1960, **187**, 186.
15 K. Manabe and K. Nakano, *Nippon Kikai Gakkai Ronbunshu, C-hen*, 2006, **72**, 3947.
16 G. Xu, T. Yamada, K. Otsubo, S. Sakaida and H. Kitagawa, *J. Am. Chem. Soc.*, 2012, **134**, 16524.
17 N. M. Bouvier and P. Palese, *Vaccine*, 2008, **26**, D49.